Journal of Mineral Resources Engineering, 7(3): 1-18, (2022)

Imam Khomeini International University

Vol. 7, No. 3, Autumn 2022

نشریه مهندسی منابع معدنی

Journal of Mineral Resources Engineering (JMRE)

Research Paper

Inversion of Magnetometric Data in the Presence of Remanent Magnetization

Ghalehnoee M.H.[1], Ansari A.[2*]

1- Ph.D, Dept. of Mining and Metallurgical Engineering, Yazd University, Yazd, Iran

2- Associate Professor, Dept. of Mining and Metallurgical Engineering, Yazd University, Yazd, Iran

Received: 16 Feb. 2021 **Accepted: 30 May 2021**

Abstract: Remanent magnetization is impossible to ignore in many applications of magnetic method including mineral exploration particularly iron ore, geomagnetism, regional investigation, and archaeological measurements. Magnetization vector inversion has made great attention in recent years since both distribution of the magnitude and direction of the magnetization have been obtained, therefore, it is easy to distinguish between different bodies especially when magnetic data are affected by remanent magnetization. In this research, the magnetization vector inversion (MVI) has presented: a 3D magnetic modelling is proposed from surface measurements to obtain magnetization distribution. The equations have solved in data-space least square to reduce computer memory requirements and speed up calculations. The algorithm has included the combination of three weights as depth weighting, distance weighting and compactness weighting in Cartesian direction. The method has been validated with a synthetic example including a dipping dyke and the results are acceptable compare with true magnetic anomaly.

Keywords: Magnetometry, Inversion, Remanent magnetization, Magnetization vector.

How to cite this article

Ghalehnoee, M. H., and Ansari, A. (2022). *"Inversion of magnetometric data in the presence of remanent magnetization"*. Journal of Mineral Resources Engineering, 7(3): 1-18.

DOI: 10.30479/JMRE.2021.15087.1491

*Corresponding Author Email: *h.ansari@yazd.ac.ir*

INTRODUCTION

Remanent magnetization is the presence of permanent magnetization in the subsurface bodies which is independent of Earth's inducing magnetic field. In many cases, strong remanent magnetization can be present and often has an unknown direction which significantly different from the direction of the inducing field.

Li [1] discussed significant advances have made in the inversion of magnetic data in the presence of significant remanent magnetization. In general, there are three strategies for inversion of magnetic data with respect to remanent magnetization: 1) inversion with direction estimation of the magnetization vector, 2) inversion by transforming magnetic data into another data that is insensitive to magnetization direction and 3) Magnetization Vector Inversion (MVI).

Given the magnetization vector values in three Cartesian directions, the inclination and declination of the magnetization vector can be easily calculated. The equations are same as Kubota and Uchiyama [2] but inversion solved in Data-Space least square algorithm. The advantages of this method are its high speed of execution and relatively good coherence of the magnetization directions. This method is validated with a synthetic example, which is simple with dipping dyke.

METHODOLOGY

Within an isotropic low-susceptibility bodies (e.g. k < 0.1 SI), the total magnetization **J** is equal to the vector sum of induced magnetization $\mathbf{J}_i$ and remanent magnetization $\mathbf{J}_r$, expressed as:

$$\mathbf{J} = \mathbf{J}_i + \mathbf{J}_r = k\mathbf{H}_o + \mathbf{J}_r \tag{1}$$

Where:

$\mathbf{H}_o$: the geomagnetic field

k : is the magnetic susceptibility, which is assumed to be isotropic throughout this paper.

The observed total magnetic field, the linear observation equation written as

$$\mathbf{T} = \mathbf{Gm} \tag{2}$$

Where:

G: the field anomaly matrix

m: is the model parameter adjustment vector. The components of the model parameter vector (**m**) written as

$$\mathbf{m} = \left(J_{x1}, J_{y1}, J_{z1}, J_{x2}, J_{y2}, J_{z2}, \ldots, J_{xM}, J_{yM}, J_{zM}, \right)^t \tag{3}$$

Where:

t: the transposition operator

G: is a N×3M matrix (N and M is the number of data and parameter respectively) with the components given by

$$\mathbf{G} = \begin{bmatrix} Gx_{11}\ Gy_{11}\ Gz_{11} & \cdots & Gx_{1M}\ Gy_{1M}\ Gz_{1M} \\ Gx_{21}\ Gy_{21}\ Gz_{21} & \cdots & Gx_{2M}\ Gy_{2M}\ Gz_{2M} \\ \vdots & \vdots & \vdots \\ Gx_{N1}\ Gy_{N1}\ Gz_{N1} & \cdots & Gx_{NM}\ Gy_{NM}\ Gz_{NM} \end{bmatrix} \tag{4}$$

The components of magnetic field anomaly are more described by Liu et al. [3].

Solving equation 2 requires minimization of the total objective function [4],

$$2S(\mathbf{m}) = \|\mathbf{T} - \mathbf{Gm}\|^2_{Wd} + \|\mathbf{m} - \mathbf{m}_o\|^2_{Wm} = (\mathbf{T} - \mathbf{Gm})^{\boldsymbol{t}}\mathbf{W}\mathrm{d}^{-\mathbf{1}}(\mathbf{T} - \mathbf{Gm}) + (\mathbf{m} - \mathbf{m}_{\boldsymbol{o}})^{\boldsymbol{t}}\mathbf{W}\mathrm{m}^{-\mathbf{1}}(\mathbf{m} - \mathbf{m}_{\boldsymbol{o}}) \tag{5}$$

Minimizing the total objective function in equation 5, yields an iterative algorithm in the data -space [4]

$$\mathbf{m}_{\boldsymbol{k}} = \mathbf{m}_{\boldsymbol{o}} + Wm_{\boldsymbol{k}}\mathbf{G}^{\boldsymbol{t}}(\mathbf{GW}\mathrm{m}_{\boldsymbol{k}}\mathbf{G}^{\boldsymbol{t}} + \mathbf{W}\mathrm{d}_{\boldsymbol{k}})^{-\mathbf{1}}(\mathbf{T}_{\boldsymbol{obs}} - \mathbf{G}\mathbf{m}_{\boldsymbol{o}}) \tag{6}$$

Where:

k: the number of iterations

$\mathbf{T}_{obs}$: denotes the measured data and the model weighting matrix $\mathbf{W}_{\mathrm{m}}$ consists of three matrices as depth-weighting function $\mathbf{W}_z$, distance matrix $\mathbf{W}_{dis}$, and compactness matrix $\mathbf{W}_c$,

$$\mathbf{C}_k = \mathbf{W}_z \mathbf{W}_{dis} \mathbf{W}_{c(k)} \tag{7}$$

The depth weighting matrix $\mathbf{W}_z$ represents a diagonal matrix whose nonzero elements are given by

$$wz_{jj} = (z_j + h)^3 \tag{8}$$

Where:
z_j: the depth of j-th voxel
h: is measurement height [5].
$\mathbf{W}_{dis}$ introduced based on [6] a diagonal matrix whose nonzero elements are given by

$$wdis_{jj} = \left(sqrt(\sum_{i=1}^{N} (R_{ij} + R_o)^2) \right)^{-1} \tag{9}$$

$\mathbf{W}c_k$ represents a diagonal matrix whose nonzero elements in k-th iteration are given by

$$wc_j^k = ((J_j^k)^2 + \varepsilon^2)^{0.5} \quad , \quad j = 1, 2, 3, \dots, M \tag{10}$$

Where $J_j = (Jx_j^2 + Jy_j^2 + Jz_j^2)^{1/2}$ is magnetization magnitude of the model in j-th voxel.

Accordingly, the model weighting matrix $\mathbf{W}\mathrm{m}_k$ ($3M \times 3M$) and $\mathbf{W}\mathrm{d}_k$ [7] in k th iteration is given

$$\mathbf{C}_k = \begin{bmatrix} \mathbf{W}_z \mathbf{W}_{dis} \mathbf{W}_{c(k)} & \mathbf{0} & \mathbf{0} \\ \mathbf{0} & \mathbf{W}_z \mathbf{W}_{dis} \mathbf{W}_{c(k)} & \mathbf{0} \\ \mathbf{0} & \mathbf{0} & \mathbf{W}_z \mathbf{W}_{dis} \mathbf{W}_{c(k)} \end{bmatrix} \tag{11}$$

$$\mathbf{W}\mathrm{d}_k = \mu^2 \times diag(\mathbf{G}\mathbf{W}\mathrm{m}_k \mathbf{G}^T) \tag{12}$$

Where $\mu > 0$ is damping factor or regularization parameter which its value depends on the noise level associated with measured data, and $\mathbf{W}\mathrm{m}_k$ is data-error weighting matrix in k-th iteration.

INVERSION OF SYNTHETIC DATA

To illustrate the efficiency of the proposed approach, the algorithm was tested using a synthetic example includes a dipping dyke with 45° west and 100 m top depth (Figure 1). Magnetization of the body is 2 A/m (0.05 SI) with magnetization inclination and declination of -25° and 330° respectively. The ambient field has strength of 50,000 nT, with a geomagnetic inclination 50° and declination 5°. The data set of the example are observed over a 21x17 grid of 50m spacing and contaminated with pseudorandom Gaussian noise with zero mean and a standard deviation of 5 nT (10% noise).

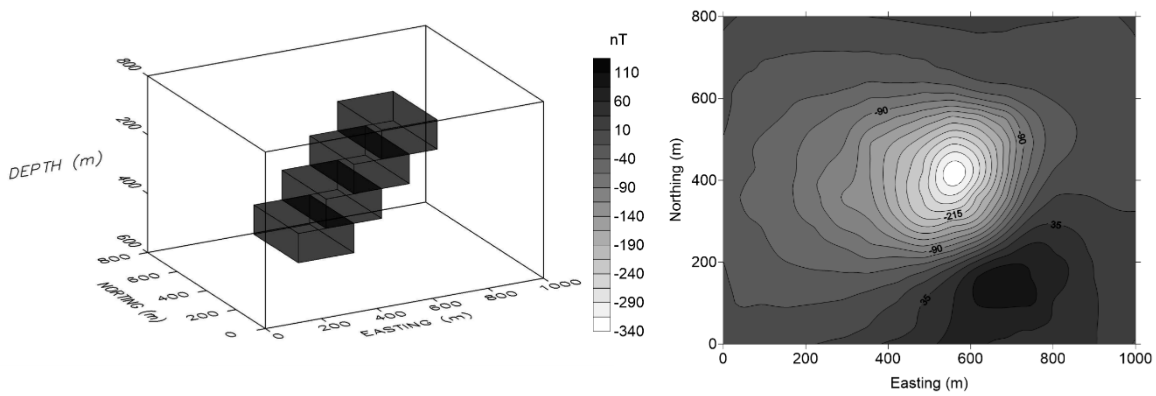

(A) **(B)**

Figure 1. Synthetic example; **A:** a dipping dyke with 45° west and 100 m top depth; magnetization of the body is 2 A/m (0.05 SI), **B:** the magnetic data with magnetization inclination and declination of -25° and 330° respectively (The ambient field has strength of 50,000 nT, with a geomagnetic inclination 50° and declination 5°.)

The example is inverted using cubic voxels with the size of 30m in 15 iterations and $\mu = 0.3$. The cone-plot of the models and volume-rendered inversion results of the recovered effective susceptibility with the cut-off at 0.02 SI also recovered (Figure 2). In Figure 2, directions of the cones near the surface and the edge of the bodies are a bit disorder and as the depth increases, the direction of the cones becomes more regular and closer to real model. This condition is due to sparsity near the surface but, the overall recovered magnetization or susceptibility model even near the surface is acceptable. In order not to face this problem and to recover more reliable inversion, especially with outcropped magnetic bodies (ore body), a few upward-continuing is proposed.

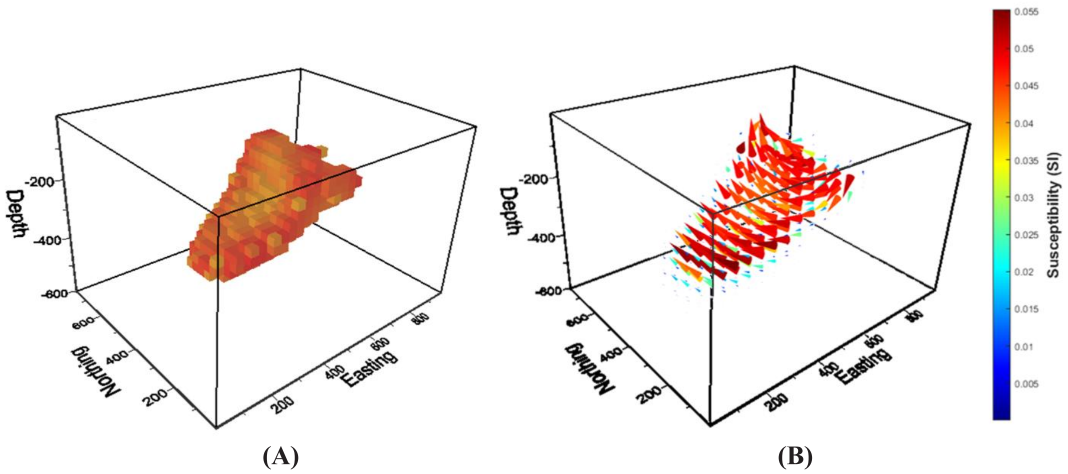

Figure 2. Inversion of the data in Figure1; **A:** volume-rendered inversion results of the recovered effective susceptibility with the effective susceptibility cut-off at 0.02 SI, **B:** magnetization vector inversion as cone-plot with the size of the cone indicates the value of effective susceptibility

CONCLUSION

In this study, we presented the magnetization vector inversion process by minimizing the total objective function in data-space method. The proposed model weighting function integrates the depth weighting, compact weighting, and distance weighting functions into the inversion process. After modeling synthetic data and proving its validation, the Shavaz magnetic data was inverted and, the model presented here three separated magnetic body with two magnetization directions. The inversion give quite acceptable results compared to the information obtained from drilling and also two different anomaly was recovered.

REFERENCES

[1] Li, Y. (2017). *"From Susceptibility to Magnetization: Advances in the 3D Inversion of Magnetic Data in the Presence of Significant Remanent Magnetization"*. Edited by Tschirhart, V., and Thomas, M. D., Proceedings of Exploration 17: Sixth Decennial International Conference on Mineral Exploration, 239-260.

[2] Kubota, R., and Uchiyama, A. (2005). *"Three-dimensional magnetization vector inversion of a seamount"*. Earth Planets Space, 57: 691-699.

[3] Liu, S., Hu, X., Zhang, H., Geng, M., and Zuo, B. (2017). *"3D magnetization vector inversion of magnetic data: improving and comparing methods"*. Pure and Applied Geophysics, 174: 4421-4444.

[4] Tarantola, A. (1987). *"Inverse problem theory"*. Elsevier Science.

[5] Li, Y., and Oldenburg, D. W. (1996). *"3D inversion of magnetic data"*. Geophysics, 61: 394-408.

[6] Li, Y., and Oldenburg, D. W. (2000). *"Joint inversion of surface and three-component borehole magnetic data"*. Geophysics, 65: 540-552.

[7] Last, B. J., and Kubik, K. (1983). *"Compact gravity inversion"*. Geophysics, 34: 65-74.